Signal Peptide Peptidase: Biochemical Properties and Modulation by Nonsteroidal Antiinflammatory Drugs†

Toru Sato,‡ Andrew C. Nyborg,§ Nobuhisa Iwata,|| Thekla S. Diehl,‡ Takaomi C. Saido,|| Todd E. Golde,§ and Michael S. Wolfe*,‡

Center for Neurologic Diseases, Brigham and Women's Hospital and Harvard Medical School, Boston, Massachusetts 02115, Department of Neuroscience, College of Medicine, Mayo Clinic, Jacksonville, Florida 32224, and Laboratory for Proteolytic Neuroscience, RIKEN Brain Science Institute, Wako-shi, Saitama 351-0198, Japan

Received March 27, 2006; Revised Manuscript Received May 11, 2006

ABSTRACT: Signal peptide peptidase (SPP) is an intramembrane aspartyl protease that cleaves remnant signal peptides after their release by signal peptidase. SPP contains active site motifs also found in presenilin, the catalytic component of the γ-secretase complex of Alzheimer's disease. However, SPP has a membrane topology opposite that of presenilin, cleaves transmembrane substrates of opposite directionality, and does not require complexation with other proteins. Here we show that, upon isolation of membranes and solubilization with detergent, the biochemical characteristics of SPP are remarkably similar to γ-secretase. The majority of the SPP-catalyzed cleavages occurred at a single site in a synthetic substrate based on the prolactin (Prl) signal sequence. However, as seen with cleavage of substrates by γ-secretase, additional cuts at other minor sites are also observed. Like γ-secretase, SPP is inhibited by helical peptidomimetics and apparently contains a substrate-binding site that is distinct from the active site. Surprisingly, certain nonsteroidal antiinflammatory drugs known to shift the site of proteolysis by γ-secretase also alter the cleavage site of Prl by SPP. Together, these findings suggest that SPP and presenilin share certain biochemical properties, including a conserved drug-binding site for allosteric modulation of substrate proteolysis.

Signal peptide peptidase (SPP)[1] is an intramembrane aspartyl protease with homology to presenilin (PS), the catalytic component of γ-secretase (*1*). SPP performs the intramembrane cleavage of membrane protein signal sequences with type II orientation (N- to C-terminus from the cytosol to the ER lumen). Such processing of the major histocompatibility complex (MHC) class I signal sequence plays a role in immune surveillance by generating human leukocyte antigen E epitopes (*2*). SPP activity is also critical for the maturation of a core protein of the hepatitis C virus, suggesting that SPP may be a suitable target for antiviral therapy (*3*). SPP contains YD and LGLGD motifs within adjacent transmembrane domains, similar to those found in PS, which as part of the γ-secretase complex produces the amyloid-β protein (Aβ) of Alzheimer's disease, and these motifs are believed to comprise the active site (*4*). However, the orientation of the active site-containing transmembrane regions of SPP is apparently opposite to that of γ-secretase (*1*, *5*, *6*). The flipped membrane orientation of SPP vis-à-vis PS correlates with the orientation of their respective substrates: γ-secretase substrates have a type I membrane topology, and SPP substrates are type II.

Despite the opposite membrane orientation with respect to PS, SPP is inhibited by transition-state analogue inhibitors of γ-secretase (*7*), suggesting that the structures of the active sites of SPP and γ-secretase are similar. Another common feature is that γ-secretase and SPP both require prior cleavage of the substrate, which is performed by α- or β-secretase and signal peptidase (*8*), respectively. Along with these similarities, SPP and γ-secretase display important differences. The activity of γ-secretase is not reconstituted in yeast, which lacks γ-secretase activity, without the coexpression of PS, nicastrin, Aph-1, and Pen-2 (*9*), whereas expression of human SPP in yeast reconstituted the protease activity (*1*), suggesting that SPP has activity on its own and does not require additional proteins. Moreover, unlike PS, SPP apparently does not undergo endoproteolysis into two associated pieces during maturation and activation. Thus, SPP is a simpler intramembrane aspartyl protease compared to γ-secretase; however, much remains unclear about the degree of biochemical similarity between these two membrane-embedded enzymes.

In the present study, we developed an in vitro cell-free SPP assay system using *n*-dodecyl β-D-maltoside (DDM) solubilized membrane fractions and a synthetic substrate, based on the prolactin (Prl) signal sequence, to analyze biochemical characteristics of SPP and discern consensus

† This work was supported by NIH Grant AG17574 (to M.S.W.), by a research fellowship from the Uehara Memorial Foundation (to T.S.), and Grant-in-Aids for Scientific Research on Priority Areas, Research on Pathomechanisms of Brain Disorders, from the Ministry of Education, Culture, Sports, Science, and Technology of Japan (17025046, 18023037) (to N.I.).

* To whom correspondence should be addressed. Tel: (617) 525-5511. Fax: (617) 525-5252. E-mail: mwolfe@rics.bwh.harvard.edu.

‡ Brigham and Women's Hospital and Harvard Medical School.

§ Mayo Clinic.

|| RIKEN Brain Science Institute.

[1] Abbreviations: Aβ, amyloid-β protein; APP, β-amyloid precursor protein; CHO, Chinese hamster ovary; DDM, *n*-dodecyl β-D-maltoside; FAD, familial Alzheimer's disease; MALDI-TOF, matrix-assisted laser desorption/ionization time of flight; NSAIDs, nonsteroidal antiinflammatory drugs; Prl, prolactin; PS, presenilin; SPP, signal peptide peptidase.

10.1021/bi060597g CCC: $33.50
Published on Web 06/27/2006

features between SPP and γ-secretase. We found that the biochemical properties of SPP are even more similar to γ-secretase than previously appreciated, including the unexpected discovery that nonsteroidal antiinflammatory agents (NSAIDs) that alter the sites of cleavage by γ-secretase also shift the cleavage sites of SPP. These findings suggest that the NSAID binding site on the γ-secretase complex resides in PS and that a better understanding of how these compounds interact with SPP may ultimately provide further insight into how they interact with γ-secretase.

EXPERIMENTAL PROCEDURES

DNA Constructs and Cell Lines. Full-length human SPP was inserted into the pcDNA6-V5-His vector as previously described (*10*). SPP mutants were prepared using *PfuUltra* high-fidelity DNA polymerase (Stratagene). These vectors were transfected into Chinese hamster ovary (CHO) cells with Lipofectamine 2000 (Invitrogen) and selected with blasticidin S (Invitrogen). Monoclonal cells stably expressing human SPP variants were cultured in Dulbecco's modified Eagle's medium (DMEM) supplemented with fetal bovine serum and blasticidin S.

Preparation of Detergent-Solubilized Membrane Fractions. Cells were collected and resuspended in homogenization (H) buffer (50 mM Hepes, pH 7.0, 250 mM sucrose, 5 mM EDTA) containing complete protease inhibitor cocktail (Roche). The cells were collapsed by being passed once through a French press at 1000 psi, and cell debris and nuclei were removed at 3000*g* for 10 min. The supernatants were centrifuged at 100000*g* for 1 h, and the resultant pellets were washed with 0.1 M sodium bicarbonate (pH 11.4) and then centrifuged again. The membrane pellets were solubilized with 2% DDM in H buffer for 90 min on ice and then centrifuged at 100000*g* for 1 h. The protein concentration of the supernatant was determined with BCA protein assay reagent (Pierce).

Cell-Free SPP Assay. DDM-solubilized membrane fractions (0.25 mg/mL protein concentration, 0.25% DDM) were incubated with SPP substrate Prl-PP (1 μM) or Prl-Flag (2 μM) and protease inhibitor cocktail at 37 °C for 90 min. The reaction was stopped by placing on ice, adding SDS sample buffer (Invitrogen) containing 5% 2-mercaptomethanol, and incubating at 37 °C for 15 min. Products were separated with 15% Tris/Tricine SDS gel containing 8 M urea, transferred to PVDF membrane (Bio-Rad), and detected with anti-myc antibody (Invitrogen). For the isolated SPP assay, the solubilized membrane fraction was incubated with anti-polyhistidine antibody (Sigma) and protein G Sepharose (Amersham) overnight. Beads with SPP were washed and resuspended in 0.25% DDM in the presence of the substrate and 0.1% phosphatidylcholine, and the samples were then assayed as described above. SPP was separated with 4−20% gel (Invitrogen) and detected with anti-SPP antibody (Abcam).

Inhibitor Treatment. Reaction mixtures were incubated in the presence of SPP inhibitors, $(Z\text{-}LL)_2$-ketone (Calbiochem) or ES2 (manuscript in preparation), γ-secretase inhibitor III-31-C (*11*), or nonsteroidal antiinflammatory drugs (NSAIDs). Sulindac sulfide (Biomol), aspirin (Sigma), and naproxen (Biomol) were dissolved in DMSO. Indomethacin (Sigma) was dissolved in ethanol. Reaction mixtures were preincubated on ice for 15 min and then placed at 37 °C. DMSO or ethanol was used as a vehicle control. The final concentration of vehicle was 1%.

Mass Spectrometric Analysis. After the incubation described above, the reaction mixture was rocked with anti-myc antibody and protein G Sepharose overnight. The resultant pellets were washed, and the immunoprecipitated samples were eluted with 1% trifluoroacetic acid/30% acetonitrile and then subjected to matrix-assisted laser desorption/ionization time-of-flight (MALDI-TOF) mass spectrometric analysis with a Voyager-DE STR Biospectrometry Workstation (Applied Biosystems). Sinapinic acid or α-cyano-4-hydroxycinnamic acid was used as a matrix. To analyze the C-terminal fragment of Prl-Flag, the supernatants were further immunoprecipitated with anti-Flag M2 antibody (Sigma) overnight and analyzed as described above.

Photolabeling of SPP. CHAPSO-solubilized membrane fractions were incubated with 5 μM biotinylated affinity probe III-63 (*12*) for 1 h in the presence of III-31-C (50 μM), $(Z\text{-}LL)_2$-ketone (20 μM), or ES2 (50 μM) and then irradiated for 45 min at 350 nm. Irradiated samples were mixed with RIPA buffer and rocked with immobilized streptavidin (Pierce) overnight. Biotinylated proteins were eluted with SDS sample buffer by incubating at 37 °C for 15 min. The samples were subjected to SDS−PAGE and western blotting, detecting with anti-V5 antibody (Invitrogen).

RESULTS

Evaluation of a Cell-Free SPP Assay System. To study proteolysis by SPP, we used synthetic bovine prolactin signal peptide (Prl) as substrate. The Prl peptide contains a myc tag on the N-terminus to detect the resultant products conveniently (Figure 1A). We used two different versions of this myc-tagged Prl, one with the natural Prl sequence and another with two proline mutations (Prl-PP) to prevent potential processing by signal peptidase (*8*), which might confound analysis of SPP proteolysis. Using DDM-solubilized membranes from CHO cells stably transfected with V5-6×His-tagged human SPP, we found that both substrates were cleaved by a protease activity that could be completely blocked by peptidomimetic $(Z\text{-}LL)_2$-ketone, a relatively specific inhibitor for SPP (*13*). However, Prl-PP was more efficiently processed than Prl, and the resultant myc-tagged N-terminal product was better separated from Prl-PP than from Prl in a Tris/Tricine urea gel (Figure 1B). On the basis of these observations, we used Prl-PP in assays designed to characterize SPP activity.

First, we used several different detergents to solubilize membrane fractions. We found that Triton X-100 and digitonin were incompatible with proteolytic processing of the Prl-PP substrate. In contrast, proteolytic activity in CHAPS- and CHAPSO-solubilized membrane fractions was not completely inhibited by $(Z\text{-}LL)_2$-ketone (data not shown), suggesting that these detergents allowed processing of Prl-PP by proteases other than SPP. We subsequently found that DDM solubilization resulted in the most efficient processing of Prl-PP and eliminated background activities, including γ-secretase. Indeed, previous studies from our laboratory have shown that the γ-secretase complex is dissociated in the presence of DDM, with concomitant loss of proteolytic

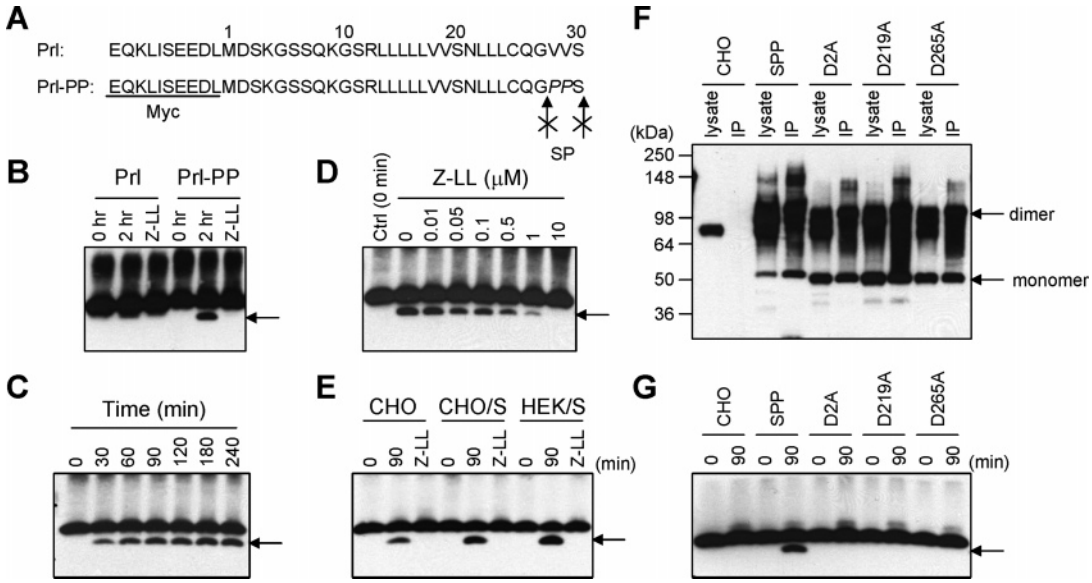

FIGURE 1: Characterization of a cell-free SPP assay system. (A) Signal sequence of bovine prolactin (Prl) and mutant Prl (Prl-PP). Arrows indicate signal peptidase (SP) cleavage sites. The myc epitope tag is underlined. Numbering is according to the Prl sequence. (B) Comparison of Prl and Prl-PP proteolysis by SPP. Solubilized membrane fractions from CHO cells stably overexpressing human SPP were incubated for 2 h in the presence or absence of 10 μM $(Z\text{-}LL)_2$-ketone (Z-LL). Proteolytic products from Prl (arrow) were detected with anti-myc antibody. (C) Time dependence of proteolytic product formation. The production plateaus after 120 min. (D) Inhibitory profile of $(Z\text{-}LL)_2$-ketone. Solubilized membrane fractions were incubated for 90 min in the presence of various concentrations of $(Z\text{-}LL)_2$-ketone. (E) SPP activity in various membrane fractions. CHO represents solubilized membrane fractions from untransfected CHO cells. CHO/S and HEK/S represent solubilized membrane fractions from CHO or HEK cells stably expressing exogenous human SPP. (F) Immunoprecipitation of SPP. SPP was immunoprecipitated with anti-polyhistidine antibody and detected by western blotting with anti-SPP antibody for SPP C-terminal amino acids. Lysate indicates solubilized membrane fractions. IP indicates immunoprecipitated complexes. SPP, D2A, D219A, and D265A represent cells expressing wild-type SPP, D219A/D265A SPP, D219A SPP, and D265A SPP, respectively. (G) Evaluation of proteolytic activity in the immunoprecipitated complexes. Only immunoprecipitated wild-type human SPP showed activity. Results shown in each panel are representative of at least two independent experiments.

activity (*14*). In DDM, proteolysis of Prl-PP plateaued at 120 min at 37 °C (Figure 1C) and was completely inhibited by $(Z\text{-}LL)_2$-ketone, with an IC_{50} value of ~100 nM (Figure 1D). γ-Secretase inhibitors DAPT (*7*) and compound E did not inhibit this proteolysis (data not shown). DDM-solubilized membrane fractions of CHO cells expressing human SPP generated the same size products as those of nontransfected CHO cells, and membranes from SPP-transfected cells processed more substrate than membranes from nontransfected cells (Figure 1E). Moreover, solubilized membrane fractions from HEK293 cells expressing human SPP generated the same size products as membranes from CHO cells (i.e., these results do not vary with the cell type). We further confirmed that the recombinant γ-secretase substrate C100Flag (*11*) was not cleaved under these conditions, demonstrating that γ-secretase is indeed inactivated and that SPP cannot cleave C100Flag (data not shown).

To fully confirm that these products were generated by SPP, we immunoprecipitated SPP using anti-polyhistidine antibody and then assayed the resultant pellets. The immunoprecipitates contained monomeric and dimeric His-tagged human SPP, as previously reported (*10*); however, endogenous SPP from untransfected CHO cells was not precipitated with the anti-polyhistidine antibody (Figure 1F). Prl cleavage products were generated from the immunoprecipitated pellets containing wild-type human SPP but not from those containing D219A and/or D265A SPP mutants (in which the active site aspartates are mutated to alanine) (Figure 1G). These results demonstrate the direct dependence of Prl-PP proteolysis on active SPP.

Identification of the Cleavage Sites of Prl. γ-Secretase cleaves at several sites within the β-amyloid precursor protein (APP) and produces secreted Aβ peptides ranging from 38 to 43 residues (*15*). To determine whether SPP cleaves at several sites similar to γ-secretase, we identified the exact cleavage sites of Prl-PP and Prl by SPP using MALDI-TOF mass spectrometry. The products from Prl-PP were immunoprecipitated with anti-myc antibody and then subjected to mass spectrometric analysis. This analysis revealed several cleaved products, whose production was almost completely inhibited by $(Z\text{-}LL)_2$-ketone, with the main cleavage site apparently being between Leu-23 and Leu-24 (Figure 2A). Because signal peak intensity cannot be quantified by MALDI-TOF mass spectrometry, we attempted to confirm the identity of the main product using Tris/Tricine urea gel. Myc-tagged Prl17, Prl20, and Prl23 were synthesized and used as standard products for the western blotting. Interestingly, as observed with Aβ peptides, shorter species of Prl-PP products migrated slower in the urea gel system (*16*) (Figure 2B). In these studies, the main product generated by the solubilized membrane fraction and by immunoprecipitated SPP (see Figure 1G) comigrated with the synthesized Prl23.

γ-Secretase cleaves APP not only in the middle of the transmembrane domain at the γ-cleavage site to produce Aβ but also seven to nine residues downstream at the ϵ-cleavage site to release the intracellular domain (*17*). However, it is unknown whether SPP similarly cleaves at two sites or not. To determine this, we used Prl containing a Flag epitope tag at the C-terminus (Prl-Flag) in order to isolate the C-terminal cleavage products with anti-Flag antibody (Figure

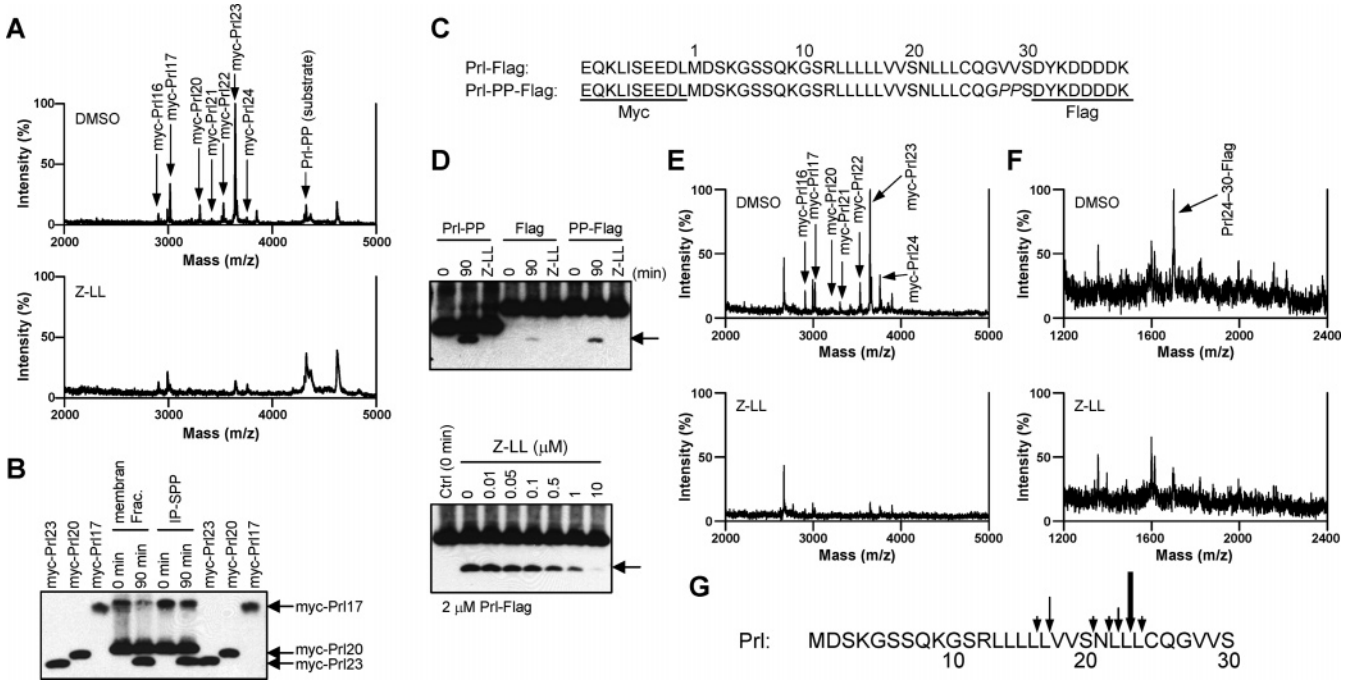

FIGURE 2: Identification of the cleavage sites of Prl by mass spectrometric analysis. (A) Representative mass peaks of Prl products from solubilized membrane fractions of wild-type SPP treated with 10 μM $(Z\text{-}LL)_2$-ketone (Z-LL) or DMSO vehicle. The N-terminal peptides are fused with the myc epitope tag. Mass numbers of N-terminal fragments are shown in Table 1. (B) Products of Prl proteolysis and standard peptides Prl17, Prl20, and Prl23 fused with myc epitope tag were separated with Tris/Tricine urea gel. The main product was Prl23 in both solubilized membrane fractions and immunoprecipitated SPP. The position of Prl17 partially overlapped with aggregated substrates. (C) Signal sequence of bovine prolactin fused with a myc epitope tag at the N-terminus and a Flag epitope tag at the C-terminus. Numbering is according to the Prl sequence. (D) Evaluation of proteolysis of 1 μM Prl-Flag by SPP. Prl-Flag is a poor substrate for SPP due to the Flag tag at the C-terminus. (E, F) Mass spectrometric analyses of N-terminal and C-terminal proteolytic fragments from Prl-Flag. Solubilized membrane fractions were treated with 10 μM $(Z\text{-}LL)_2$-ketone (Z-LL) or DMSO vehicle. Mass numbers of C-terminal fragments are shown in Table 1. Results shown in each panel are representative of at least two independent experiments. (G) Schematic representation of bovine Prl cleavage sites. SPP cleaves predominantly between Leu-23 and Leu-24.

Table 1: Prl Products in a Cell-Free Assay System

Prl no.	M_r (obsd)	M_r (calcd)
N-terminal		
myc-Prl16	2905.80	2906.32
myc-Prl17	3019.03	3019.48
myc-Prl20	3304.65	3304.82
myc-Prl21	3418.84	3418.93
myc-Prl22	3532.74	3532.09
myc-Prl23	3645.27	3645.24
myc-Prl24	3757.14	3758.41
C-terminal		
Prl24−30Flag	1700.80	1700.81

2C). We found that these Flag-tagged substrates were cleaved with extremely poor efficiency, although the double proline mutant substrate (Prl-PP-Flag) was processed by SPP more effectively than Prl-Flag (Figure 2D). The IC_{50} value of $(Z\text{-}LL)_2$-ketone for inhibiting cleavage of the Prl-Flag substrate was slightly higher (~700 nM) than Prl-PP. A previous report showed that an ~27-residue fragment of Prl appeared in the presence of $(Z\text{-}LL)_2$-ketone, and the authors suggested that this fragment was generated by signal peptidase (*13*). However, in DDM-solubilized membranes using the Prl-Flag substrates, signal peptidase activities were not revealed in the presence of $(Z\text{-}LL)_2$-ketone (Figure 2D), suggesting that this Prl substrate is cleaved only by SPP in this system.

We first analyzed N-terminal products by MALDI-TOF mass spectrometry using Prl-Flag. Although the relative height of the Prl24 peak produced from Prl-Flag was somewhat higher than that produced from Prl-PP, all of the same N-terminal fragments appeared from Prl-Flag that were observed from Prl-PP, and the main product generated from Prl-Flag was likewise Prl23 (Figure 2E). The generation of these fragments was dramatically reduced by $(Z\text{-}LL)_2$-ketone. We also analyzed the C-terminal cleavage products by MALDI-TOF mass spectrometry after immunoprecipitation with anti-Flag antibody. Only one peak clearly appeared, identified as Prl24−30, which did not appear in the presence of $(Z\text{-}LL)_2$-ketone (Figure 2F). This C-terminal fragment was exactly complementary to the main N-terminal cleavage product (Prl23). Other minor C-terminal fragments were not detectable. We also confirmed the identity of the proteolytic products using an N-terminal HA tag (instead of myc tag) on the wild-type Prl substrate; the cleavage sites were the same, and the main product was likewise Prl23 (data not shown), indicating that neither the epitope tag nor the proline mutations influence the sites of proteolysis. Taken together, these results suggest that SPP cleaves mainly at one site, although a limited degree of heterogeneous proteolysis takes place, which may reflect double cleavage (Figure 2G).

Evidence That SPP Has a Substrate-Binding Site That Is Distinct from the Active Site. γ-Secretase contains an initial binding site (docking site) for the substrate transmembrane domain that is distinct from the active site, and this site resides on PS and not other members of the protease complex (*18*). Key to the identification of this docking site was helical peptide inhibitors based on the transmembrane domain of the APP. To determine whether SPP contains such a docking site, we designed a helical peptide inhibitor (ES2) based on

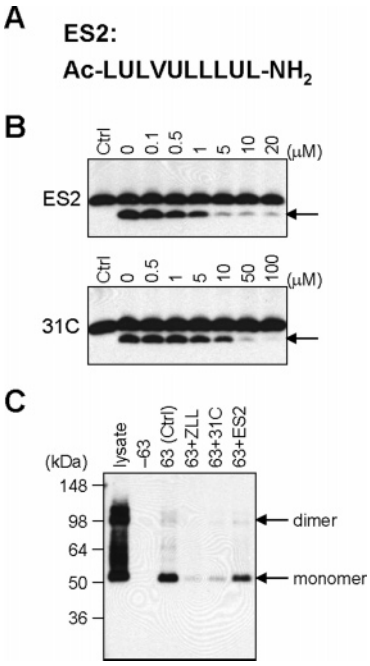

FIGURE 3: Photolabeling of SPP and competition with a helical inhibitor. (A) Chemical structure of the helical peptide SPP inhibitor. U indicates α-aminoisobutyric acid, a helix-inducing residue. (B) Inhibitory potencies of ES2 and III-31C. IC_{50} values of ES2 and III-31C were ~1 and ~10 μM, respectively. (C) The helical inhibitor binds to a location distinct from the active site. SPP was photolabeled with 5 μM biotinylated affinity probe III-63 (Ctrl). The absence of III-63 (−63) served as a control. Photolabeled SPP was blocked by 20 μM $(Z\text{-}LL)_2$-ketone (63 + ZLL) or 50 μM III-31C (63 + 31C); however, labeling was not prevented by 50 μM ES2 (63 + ES2). Results shown in each panel are representative of at least two independent experiments.

the Prl signal sequence. This peptide contains 10 residues from the Prl sequence, with every third or fourth residue replaced with the helix-inducing α-aminoisobutyric acid (U; Figure 3A). This peptide inhibited SPP activity with an IC_{50} value of ~1 μM (Figure 3B), a higher potency than III-31-C (~10 μM), a transition-state analogue inhibitor of γ-secretase that we previously showed could also inhibit SPP (*5*). Inhibitor III-31-C is the parent compound of III-63, a photoactivable biotinylated affinity labeling reagent for both γ-secretase (*12*) and SPP (*10*). Detergent-solubilized membrane fractions from CHO cells stably expressing human SPP were incubated with the active site-directed photoprobe III-63 (5 μM) in the presence of several inhibitors and subjected to UV irradiation. After pulling down photolabeled SPP with streptavidin beads, samples were analyzed for the presence of SPP by western blotting. SPP was photolabeled with III-63 as we previously reported (*10*), although in this case, we observed virtually all labeled SPP as a monomer: little or no labeled SPP dimer was seen. The reason for this discrepancy is not clear, but one possibility is disruption of the dimer during the photolabeling process. In any case, this labeling was specific, as it was blocked with two different transition-state analogue SPP inhibitors (Figure 3C), and should reflect interaction with the SPP active site. In contrast, an equivalent concentration (50 μM) of ES2 did not effectively block III-63 photolabeling compared to III-31-C, even though ES2 was a more potent inhibitor of SPP activity than III-31-C. These results indicate that the substrate-based helical peptide ES2 binds to a site on SPP that is distinct from the active site. This property of SPP is closely similar to that of PS in the active γ-secretase complex (*18*).

Familial Mutation like SPP Does Not Alter the Cleavage Sites. PS mutations associated with familial Alzheimer's disease (FAD) cause enhanced production of Aβ42 (*15*). Several positions where these mutations are found are also conserved in SPP (*4*). We therefore mutagenized three different positions in SPP, two of which are especially close to the presumed active site aspartates. Similar mutations in PS shift γ-secretase cleavage and elevate production of the more deleterious Aβ42 relative to Aβ40 (*19*) (Figure 4A). We prepared S82I, Y218S, and G264A human SPP, which are comparable to the T147I, Y256S, and G384A PS1 FAD mutations (*20*−*22*). The SPP mutants were expressed in stable CHO cell lines at levels comparable to exogenous wild-type human SPP and displayed normal mobilities of monomic and dimeric SPP (Figure 4B). To analyze the effect of these SPP mutations on cleavage, we first investigated the formation of proteolytic products from Prl by SDS−PAGE. DDM-solubilized membrane fractions from each mutant-expressing cell line were incubated with the Prl substrate in the presence or absence of $(Z\text{-}LL)_2$-ketone. Generation of the cleavage product in membrane fractions containing Y218S SPP was similar to those containing wild-type SPP (Figure 4C). In contrast, S82I and G264A mutant SPPs displayed partially lower proteolysis compared with wild-type SPP. We then analyzed the products by MALDI-TOF mass spectrometry for changes in cleavage site specificity, as seen with presenilins. Mass spectrometric results showed that FAD-like mutations in SPP did not affect the cleavage sites at all (Figure 4D). We also confirmed the identity of the C-terminal proteolytic fragments using Prl-Flag by MALDI-TOF mass spectrometry, and similar results were obtained (data not shown). These results demonstrate that while FAD-like mutations can affect SPP activity, these particular mutations do not alter the cleavage site specificity. FAD PS mutants, including PS1 G384A, generally cause reduced γ-secretase activity (*19*, *23*, *24*). Thus, these FAD-like mutations in SPP tend to mimic the reduction of proteolytic function seen with the corresponding PS mutations but do not change the site of proteolytic cleavage.

Nonsteroidal Antiinflammatory Drugs Modulate SPP Activity. A subset of NSAIDs is known to specifically decrease Aβ42 production while simultaneously increasing Aβ38 production (*25*). These compounds are proposed to change the conformation of γ-secretase by binding to an unidentified allosteric site on the protease complex (*26*, *27*). To investigate whether these compounds also affect SPP activity, we treated DDM-solubilized SPP-containing membranes with various NSAIDs and analyzed the products by western blotting. Both sulindac sulfide and indomethacin, which are effective modulators of γ-secretase, showed a small but consistent decrease in mobility compared to product generated in the presence of control DMSO vehicle alone (Figure 5A, left panel). In contrast, aspirin and naproxen, which do not affect γ-secretase activity, did not affect the mobility or levels of the SPP-generated Prl cleavage product. Although γ-secretase is inhibited with high concentrations of NSAIDs (*26*), SPP was not inhibited by these NSAIDs at concentrations up to 2 mM (Figure 5A, right panel). To

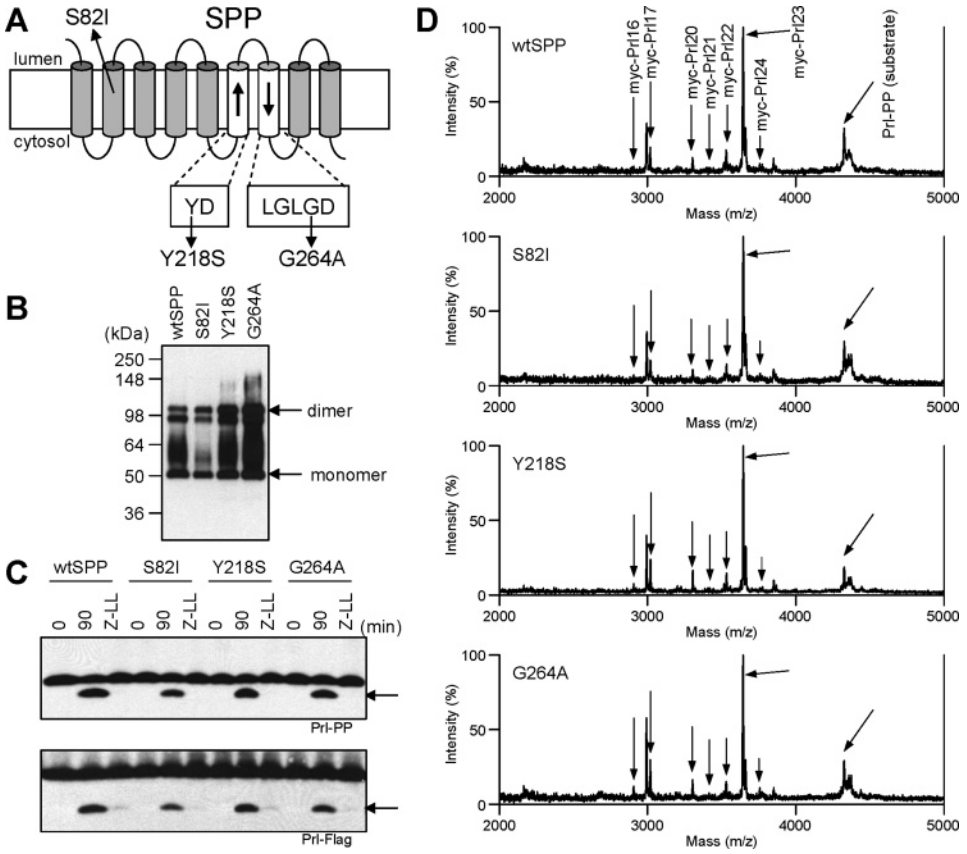

FIGURE 4: Effects of FAD-like mutations on SPP activity. (A) Schematic representation of FAD-like mutations in SPP. (B) Expression of FAD-like mutant SPP. All mutagenized SPPs are seen as both a monomer and an SDS-stable dimer. (C) Prl processing by FAD-like mutant SPPs. All mutant membrane fractions were incubated for 90 min in the presence or absence of 10 μM (Z-LL)$_2$-ketone. Both substrates, Prl-PP and Prl-Flag, were used for the assay. (D) Mass spectrometric analysis of proteolytic products generated by FAD-like mutant SPPs. The proteolytic products from Prl-PP were immunoprecipitated with anti-myc antibody and then subjected to mass spectrometric analysis. All arrows in the mass spectrometric profiles of the mutant correspond to the profile of the wild type. Results shown in each panel are representative of at least two independent experiments.

determine whether NSAIDs alter the cleavage site specificity, we performed mass spectrometric analysis of the N-terminal proteolytic products generated in the presence of NSAIDs. Remarkably, this analysis showed a clear increase in Prl24, a product one residue longer than the major product Prl23, in the presence of 500 μM sulindac sulfide or indomethacin (Figure 4B). Aspirin and naproxen did not affect cleavage site specificity. It should be noted that an important difference between the interaction of active NSAIDs with SPP vis-à-vis γ-secretase is that the SPP proteolysis is partially shifted one residue in the C-terminal direction, while γ-secretase proteolysis is shifted four residues in the N-terminal direction. The similarities are nonetheless striking despite this difference: because SPP does not form a complex with other proteins (*1*) but is affected by the same NSAIDs that modulate γ-secretase, the implication is that the NSAID binding site on the γ-secretase complex resides on PS, at a site conserved in SPP.

DISCUSSION

γ-Secretase cleaves the transmembrane domain of its substrates in two positions. This double proteolysis is exemplified by APP and Notch. APP is cleaved in the middle of the membrane at the γ site, to generate Aβ, and also closer to the cytosolic side at the ϵ site, to release the intracellular domain (*28*). Likewise, Notch is cleaved in the middle of the membrane at the S4 site and also near the cytosolic side at the S3 site, the latter cleavage releasing the intracellular domain that plays an essential role in Notch signal transduction. In contrast, we find that SPP proteolyzes predominantly in one position comparable to the ϵ/S3 cleavage site of γ-secretase, although SPP also displays heterogeneity in the N-terminal cleavage products, suggesting that a limited degree of double proteolysis may occur as well. Interestingly, SPP cleaves the Prl substrate predominantly after residue 23, but also after residues 20 and 17 (Figure 2A,E), placing the primary scissile amide bonds along one face of the α-helical substrate transmembrane domain. Although we found N-terminal cleavage products Prl17 and Prl20, we could not find their C-terminal counterparts Prl18−30 and Prl21−30. A previous study showed that the cleavage site of Prl was around Prl20 by mobility in gels (*29*). However, the method of analysis did not allow identification of the exact cleavage site and also could not reveal other minor cleavage sites. In contrast, by mass analysis, we could exactly identify all cleavage sites including minor sites.

Although SPP has the same putative aspartate-containing active site motifs as PS, the identity of the entire amino acid sequence is very low (~20%). Moreover, the topology of SPP is opposite that of PS, and consistent with this difference, SPP cleaves transmembrane substrates with a membrane orientation opposite that of γ-secretase substrates. Further, unlike PS, SPP does not require other protein partners or endoproteolysis into two subunits for proteolytic activity.

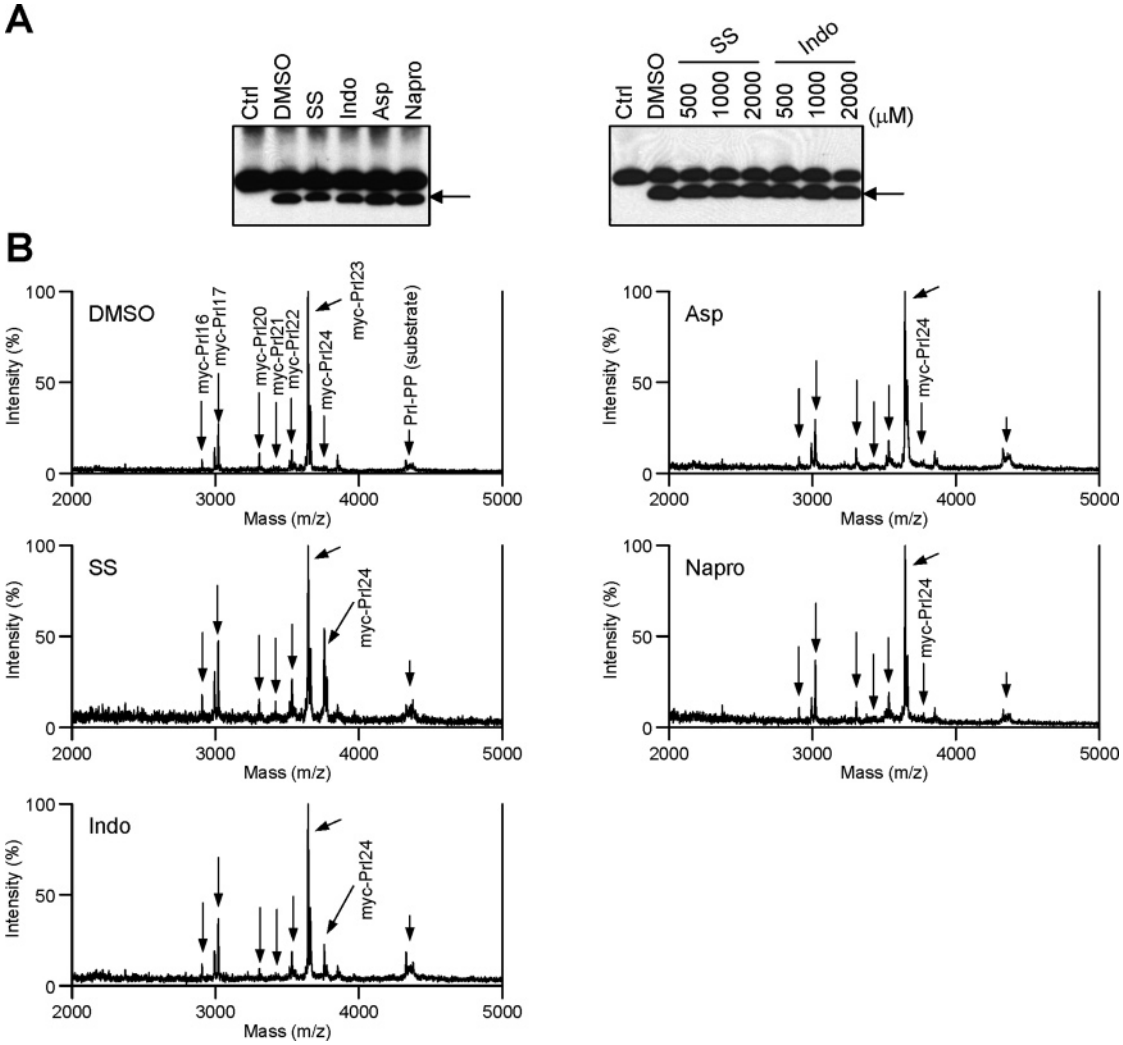

FIGURE 5: Effect of NSAIDs on SPP activity. (A) Effect of NSAIDs on overall activity. Solubilized membrane fractions were incubated for 90 min in the presence of 500 μM (left panel) or various concentrations (right panel) of sulindac sulfide (SS), indomethacin (Indo), aspirin (Asp), and naproxen (Napro), respectively. (B) Mass spectrometric analysis of proteolytic products generated by SPP in the presence of NSAIDs. The proteolytic products from Prl-PP were immunoprecipitated with anti-myc antibody and then subjected to mass spectrometric analysis. All arrows in the mass spectrometric profiles from the NSAID-treated samples correspond to the peaks seen in the profile of the wild type. Results shown in each panel are representative of at least two independent experiments.

Despite these major differences, certain similarities to γ-secretase are striking. Interestingly, proteolysis of Prl in CHAPS or CHAPSO detergents was partially blocked by dipeptide analogue DAPT, which is capable of inhibiting γ-secretase but not SPP (data not shown) (*7*). These results suggest that Prl can be processed by both γ-secretase and SPP when these two oppositely oriented proteases are solubilized out of the asymmetric context of the lipid bilayer using CHAPS or CHAPSO detergents. Both proteases have loose sequence specificity for substrates. Moreover, both SPP and γ-secretase recognize α-helical regions (Figure 3) of substrates and cleave inside these helical regions (Figure 2). On the other hand, SPP does not cleave C100Flag and cleaves Prl-Flag with low efficiency, indicating that the length or identity of the substrate C-terminus is important for the recognition or proteolysis by these proteases. We also find that SPP is inhibited by a substrate-based helical peptide that binds to a site distinct from the active site, suggesting that proteolysis by SPP likewise involves initial binding (docking) of the substrate transmembrane domain on the outer surface of the protease before entry into the internal, water-containing active site. This enzymatic mechanism, initial substrate docking and then entry into the active site, is likely a general mechanism for the emerging class of membrane-embedded proteases, including the S2P family of metalloproteases and the rhomboid family of serine proteases (*30*).

Most surprisingly, the cleavage site specificity of SPP can be altered by certain NSAIDs known to affect the cleavage site specificity of γ-secretase for its substrate APP. These changes were observed both by SDS−PAGE and by mass spectrometry. NSAIDs that do not affect γ-secretase activity also do not affect SPP activity. Such data could be accounted for by several mechanisms: (i) a common NSAID binding site conserved between PS and SPP; (ii) interaction of NSAIDs with TMD regions of γ-secretase and SPP substrates; or (iii) modulation of the membrane environment by the NSAID. Modulation of the membrane environment seems unlikely, because NSAIDs can cause these effects even in detergents below their critical micelle concentrations. Binding to the single TMD of the substrate also seems less plausible, because a single transmembrane domain can at best only have a very shallow binding pocket. Thus, we favor a conserved NSAID binding site on PS and SPP. Because certain NSAIDs

shift the production of Aβ away from the more deleterious 42-residue form, these compounds are considered an important class of potential therapeutics for Alzheimer's disease. Indeed, one such compound, R-flurbiprofen, has recently shown promise in phase II clinical trials (*31*). Elucidating how these compounds exert their effects on the cleavage site specificity of γ-secretase is crucial to developing more potent and selective agents. Our findings suggest that determining the binding site of NSAIDs on SPP, which should be much more amenable to detailed structural studies than the large and complicated γ-secretase complex, will reveal a closely related binding site on presenilin.

REFERENCES

1. Weihofen, A., Binns, K., Lemberg, M. K., Ashman, K., and Martoglio, B. (2002) Identification of signal peptide peptidase, a presenilin-type aspartic protease, *Science 296*, 2215−2218.
2. Lemberg, M. K., Bland, F. A., Weihofen, A., Braud, V. M., and Martoglio, B. (2001) Intramembrane proteolysis of signal peptides: an essential step in the generation of HLA-E epitopes, *J. Immunol. 167*, 6441−6446.
3. McLauchlan, J., Lemberg, M. K., Hope, G., and Martoglio, B. (2002) Intramembrane proteolysis promotes trafficking of hepatitis C virus core protein to lipid droplets, *EMBO J. 21*, 3980−3988.
4. Ponting, C. P., Hutton, M., Nyborg, A., Baker, M., Jansen, K., and Golde, T. E. (2002) Identification of a novel family of presenilin homologues, *Hum. Mol. Genet. 11*, 1037−1044.
5. Nyborg, A. C., Jansen, K., Ladd, T. B., Fauq, A., and Golde, T. E. (2004) A signal peptide peptidase (SPP) reporter activity assay based on the cleavage of type II membrane protein substrates provides further evidence for an inverted orientation of the SPP active site relative to presenilin, *J. Biol. Chem. 279*, 43148−43256.
6. Doan, A., Thinakaran, G., Borchelt, D. R., Slunt, H. H., Ratovitsky, T., Podlisny, M., Selkoe, D. J., Seeger, M., Gandy, S. E., Price, D. L., and Sisodia, S. S. (1996) Protein topology of presenilin 1, *Neuron 17*, 1023−1030.
7. Weihofen, A., Lemberg, M. K., Friedmann, E., Rueeger, H., Schmitz, A., Paganetti, P., Rovelli, G., and Martoglio, B. (2003) Targeting presenilin-type aspartic protease signal peptide peptidase with gamma-secretase inhibitors, *J. Biol. Chem. 278*, 16528−16533.
8. Lemberg, M. K., and Martoglio, B. (2002) Requirements for signal peptide peptidase-catalyzed intramembrane proteolysis, *Mol. Cell 10*, 735−744.
9. Edbauer, D., Winkler, E., Regula, J. T., Pesold, B., Steiner, H., and Haass, C. (2003) Reconstitution of γ-secretase activity, *Nat. Cell Biol. 5*, 486−488.
10. Nyborg, A. C., Kornilova, A. Y., Jansen, K., Ladd, T. B., Wolfe, M. S., and Golde, T. E. (2004) Signal peptide peptidase forms a homodimer that is labeled by an active site-directed γ-secretase inhibitor, *J. Biol. Chem. 279*, 15153−15160.
11. Esler, W. P., Kimberly, W. T., Ostaszewski, B. L., Ye, W., Diehl, T. S., Selkoe, D. J., and Wolfe, M. S. (2002) Activity-dependent isolation of the presenilin-γ-secretase complex reveals nicastrin and a γ substrate, *Proc. Natl. Acad. Sci. U.S.A. 99*, 2720−2725.
12. Kornilova, A. Y., Das, C., and Wolfe, M. S. (2003) Differential effects of inhibitors on the γ-secretase complex. Mechanistic implications, *J. Biol. Chem. 278*, 16470−16473.
13. Weihofen, A., Lemberg, M. K., Ploegh, H. L., Bogyo, M., and Martoglio, B. (2000) Release of signal peptide fragments into the cytosol requires cleavage in the transmembrane region by a protease activity that is specifically blocked by a novel cysteine protease inhibitor, *J. Biol. Chem. 275*, 30951−30956.
14. Fraering, P. C., LaVoie, M. J., Ye, W., Ostaszewski, B. L., Kimberly, W. T., Selkoe, D. J., and Wolfe, M. S. (2004) Detergent-dependent dissociation of active γ-secretase reveals an interaction between Pen-2 and PS1-NTF and offers a model for subunit organization within the complex, *Biochemistry 43*, 323−333.
15. Selkoe, D. J. (2001) Alzheimer's disease: genes, proteins, and therapy, *Physiol. Rev. 81*, 741−766.
16. Klafki, H. W., Wiltfang, J., and Staufenbiel, M. (1996) Electrophoretic separation of βA4 peptides (1−40) and (1−42), *Anal. Biochem. 237*, 24−29.
17. Weidemann, A., Eggert, S., Reinhard, F. B., Vogel, M., Paliga, K., Baier, G., Masters, C. L., Beyreuther, K., and Evin, G. (2002) A novel var ϵ-cleavage within the transmembrane domain of the Alzheimer amyloid precursor protein demonstrates homology with Notch processing, *Biochemistry 41*, 2825−2835.
18. Kornilova, A. Y., Bihel, F., Das, C., and Wolfe, M. S. (2005) The initial substrate-binding site of γ-secretase is located on presenilin near the active site, *Proc. Natl. Acad. Sci. U.S.A. 102*, 3230−3235.
19. Steiner, H., Kostka, M., Romig, H., Basset, G., Pesold, B., Hardy, J., Capell, A., Meyn, L., Grim, M. L., Baumeister, R., Fechteler, K., and Haass, C. (2000) Glycine 384 is required for presenilin-1 function and is conserved in bacterial polytopic aspartyl proteases, *Nat. Cell Biol. 2*, 848−851.
20. Campion, D., Dumanchin, C., Hannequin, D., Dubois, B., Belliard, S., Puel, M., Thomas-Anterion, C., Michon, A., Martin, C., Charbonnier, F., Raux, G., Camuzat, A., Penet, C., Mesnage, V., Martinez, M., Clerget-Darpoux, F., Brice, A., and Frebourg, T. (1999) Early-onset autosomal dominant Alzheimer disease: prevalence, genetic heterogeneity, and mutation spectrum, *Am. J. Hum. Genet. 65*, 664−670.
21. Miklossy, J., Taddei, K., Suva, D., Verdile, G., Fonte, J., Fisher, C., Gnjec, A., Ghika, J., Suard, F., Mehta, P. D., McLean, C. A., Masters, C. L., Brooks, W. S., and Martins, R. N. (2003) Two novel presenilin-1 mutations (Y256S and Q222H) are associated with early-onset Alzheimer's disease, *Neurobiol. Aging 24*, 655−662.
22. Cruts, M., Backhovens, H., Wang, S. Y., Van Gassen, G., Theuns, J., De Jonghe, C. D., Wehnert, A., De Voecht, J., De Winter, G., and Cras, P. (1995) Molecular genetic analysis of familial early-onset Alzheimer's disease linked to chromosome 14q24.3, *Hum. Mol. Genet. 4*, 2363−2371.
23. Song, W., Nadeau, P., Yuan, M., Yang, X., Shen, J., and Yankner, B. A. (1999) Proteolytic release and nuclear translocation of Notch-1 are induced by presenilin-1 and impaired by pathogenic presenilin-1 mutations, *Proc. Natl. Acad. Sci. U.S.A. 96*, 6959−6963.
24. Bentahir, M., Nyabi, O., Verhamme, J., Tolia, A., Horre, K., Wiltfang, J., Esselmann, H., and De Strooper, B. (2006) Presenilin clinical mutations can affect gamma-secretase activity by different mechanisms, *J. Neurochem. 96*, 732−742.
25. Weggen, S., Eriksen, J. L., Das, P., Sagi, S. A., Wang, R., Pietrzik, C. U., Findlay, K. A., Smith, T. E., Murphy, M. P., Bulter, T., Kang, D. E., Marquez-Sterling, N., Golde, T. E., and Koo, E. H. (2001) A subset of NSAIDs lower amyloidogenic Aβ42 independently of cyclooxygenase activity, *Nature 414*, 212−216.
26. Beher, D., Clarke, E. E., Wrigley, J. D., Martin, A. C., Nadin, A., Churcher, I., and Shearman, M. S. (2004) Selected nonsteroidal antiinflammatory drugs and their derivatives target γ-secretase at a novel site. Evidence for an allosteric mechanism, *J. Biol. Chem. 279*, 43419−43426.
27. Lleo, A., Berezovska, O., Herl, L., Raju, S., Deng, A., Bacskai, B. J., Frosch, M. P., Irizarry, M., and Hyman, B. T. (2004) Nonsteroidal antiinflammatory drugs lower Aβ42 and change presenilin 1 conformation, *Nat. Med. 10*, 1065−1066.
28. Kopan, R., and Ilagan, M. X. (2004) γ-Secretase: proteasome of the membrane?, *Nat. Rev. Mol. Cell Biol. 5*, 499−504.
29. Lyko, F., Martoglio, B., Jungnickel, B., Rapoport, T. A., and Dobberstein, B. (1995) Signal sequence processing in rough microsomes, *J. Biol. Chem. 270*, 19873−19878.
30. Wolfe, M. S., and Kopan, R. (2004) Intramembrane proteolysis: theme and variations, *Science 305*, 1119−1123.
31. Black, S., et al. (2005) Society for Neuroscience, Program No. 586.6.

BI060597G